

*Work supported in part by National Science Foundation.

¹J. Benecke, T. T. Chou, C. N. Yang, and E. Yen, *Phys. Rev.* **188**, 2159 (1969).

²R. P. Feynman, *Phys. Rev. Letters* **23**, 1415 (1969).

³H. Satz, *Phys. Letters* **25B**, 220 (1967).

⁴N. N. Biswas, N. M. Cason, V. P. Kenney, J. T. Powers, W. D. Shephard, and D. W. Thomas, *Phys. Rev.*

Letters **26**, 1589 (1971).

⁵J. W. Elbert, A. R. Erwin, and W. D. Walker, *Phys. Rev. D* **3**, 2042 (1971); W. Ko and R. L. Lander, *Phys. Rev. Letters* **26**, 1064 (1971).

⁶The value of p' for a given r can be calculated from the relation $(p'^2 + \mu^2)^{1/2} + (r^2 p'^2 + M^2)^{1/2} = \sqrt{s}$, and hence the quantities e_p and e_t .

PHYSICAL REVIEW D

VOLUME 6, NUMBER 11

1 DECEMBER 1972

Two-Particle Exclusive Correlations at 23 GeV/c Compared with a Diffraction Excitation and a Multiperipheral Model

D. E. Lyon, Jr. and York-Peng Yao

Physics Department, The University of Michigan, Ann Arbor, Michigan 48104

(Received 31 July 1972)

Two-particle correlations in the process $p + p \rightarrow p + p + \pi^+ + \pi^+ + \pi^- + \pi^-$ at 23-GeV/c incident momentum are analyzed with a diffraction excitation model, and a Reggeized multiperipheral model that contains symmetrization and baryon exchange. The former provides a slightly better description of the correlation data. Some single-particle distribution model calculations are presented and discussed.

INTRODUCTION

Two types of models for high-energy hadron-hadron interactions have recently received intensive treatment. One of these is the multiperipheral model (MPM),¹ and the other the diffraction excitation model (DEM).² The former asserts that at high energy nondiffractive processes dominate the total production cross section, and the latter that diffractive processes dominate. Insofar as the gross features of inclusive single-particle spectra that they predict are concerned, there is not much difference between the two at presently attainable machine energies as the parameters of each model are adjusted so that they compare well with the data. Partly for this reason, there has been much discussion of the correlation phenomena. We share the view that this is a sensitive area to investigate for the distinction of the models. However, it is also our opinion that since the inclusive cross sections are the outcome of exclusive processes, the place to unravel the details of dynamics is the exclusive process. This is because the more integration the data involve, the less sensitive to dynamical details it becomes. In this paper, therefore, we investigate the exclusive process $p + p \rightarrow p + p + \pi^+ + \pi^+ + \pi^- + \pi^-$ at 23 GeV/c.³ We compare the predictions of the aforementioned theoretical approaches with the correlation data available to us, show some single-particle distributions of interest, and demonstrate the energy dependence of these distributions.

The choice of the process (studied here) is a compromise between two requirements. First, in order to test DEM the process must truly be diffractive. From our experience, this implies that the c.m. energy available for particles in the final state to move away from each other must be a few GeV. There cannot, therefore, be too many particles present. Second, to be able to apply the statistical arguments of the diffractive model, the number of particles cannot be too few. The compromise situation is to study a reaction where the number of particles in the final state is about the same as the average multiplicity at the given energy. The process selected here for study meets these requirements. In this process, however, double excitation of the incident nucleons can occur. A reaction that would better unveil the parameters of the diffractive process would be one in which the excitation of only one of the incident particles is possible. We have studied such a process, $d + p \rightarrow d + p + \pi^+ + \pi^-$ at 25 GeV/c, and will report the results in a later publication.

DIFFRACTION EXCITATION MODEL

In the DEM considered here, two incident particles interact with each other via the exchange of a Pomeranchukon and get excited. The quasi-stable systems created then decay with the emission of pions and the original particles. The detailed dynamics of the decay may be very compli-

cated indeed, but the statistical postulate is that since many channels are open the resulting distributions are governed by the laws of probability.

$$T_n = i\beta_1(t)\beta_2(t) \sum_{i=1}^{n/2} \left(\frac{s}{M_1^2 M_2^2} \right)^{\alpha_P(t)} (M_1 M_2)^{1/2} P_{1 \rightarrow n_1} P_{2 \rightarrow n_2} \delta_{n_1+n_2, n} \delta_{n_1, 2i-1}, \quad (1)$$

where M_j is the mass of the excited state j , $P_{j \rightarrow n_j}$ is the probability amplitude for the excited nucleon j to decay into n_j final particles, $\beta_1(t)\beta_2(t)$ is the residue function on the vertices, and where for simplicity we have assumed a factorizable Pomeron. The δ functions simply express the fact that each excited state can decay only with an even number of charged pions. The factor $(M_1 M_2)^{1/2}$ expresses the assumption of a weak triple-Pomeron coupling and the consequent f -trajectory dominance.⁴

We apply statistical arguments for the decay of each excited nucleon and write

$$P_{j \rightarrow n_j} = \prod_{i=1}^{n_j} \exp(C_i |\vec{k}_i|^2), \quad (2)$$

where \vec{k}_i is the momentum of the i th decay product, in the rest frame of "fireball" j . C_i can be expected to depend somewhat on the species of particle being emitted since, experimentally, one observes that the higher-mass secondaries have larger transverse momenta. A consequence of this decay probability is that the emitted particles from each fireball will be isotropic in the rest frame of their respective fireball.

From an analysis of $p+p \rightarrow p + \text{anything}$, we find that satisfactory parametrizations of the residue function can be written as

$$\beta_1(t)\beta_2(t) = \exp \left[a \left(\frac{1}{M_1} + \frac{1}{M_2} \right) t \right] \quad (2a)$$

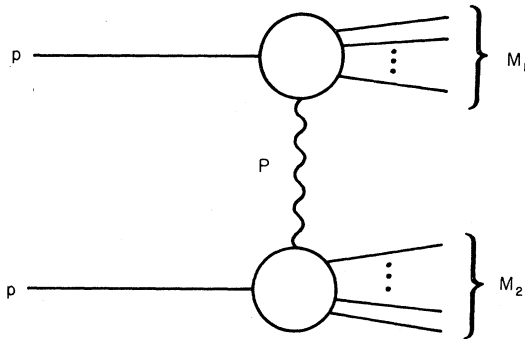


FIG. 1. Diffraction excitation model considered in this paper.

Figure 1 shows the dominant mechanism for production, in this model. The invariant matrix element representing the process is written as

or

$$\beta_1(t)\beta_2(t) = \exp \left[a' \left(\frac{1}{M_1^2} + \frac{1}{M_2^2} \right) t \right]. \quad (2b)$$

The cross section for the production of n particles is

$$d\sigma_n = \frac{|T_n|^2 d\Phi_n}{4p^* s^{1/2}}, \quad (3)$$

where $d\Phi_n$ is the Lorentz-invariant phase-space volume element for n particles in the final state and p^* is the momentum of one of the incident particles, in the center-of-mass system. Then

$$\sigma_n = \int d\sigma_n \quad (4)$$

and

$$\frac{d\sigma_n}{d\alpha} = \frac{d}{d\alpha} \int d\sigma_n, \quad (5)$$

the total inelastic cross section for the production of n particles and the differential cross section with respect to some variable α , respectively. We have evaluated these integrals numerically with a Monte Carlo phase-space integration technique.⁵ The program generates "events" in Lorentz-invariant phase space with a frequency distribution given by $|T_n|^2$. The calculations are exact and there is, therefore, no need to go to infinite s , as is usually the case, in order to make predictions. The various single particle and correlation distributions are merely projected out of the sample of "events" generated.⁶

In the process we are investigating, the excited nucleons have three decay modes:

- (1) $p \rightarrow p$,
- (2) $p \rightarrow p + \pi^+ + \pi^-$,
- (3) $p \rightarrow p + \pi^+ + \pi^+ + \pi^- + \pi^-$.

For simplicity we assume that the parameters a or a' , C_p , and C_π are independent of the decay mode. They are thus determined by fitting the observed transverse-momentum distributions of the protons and pions. Here, we find that

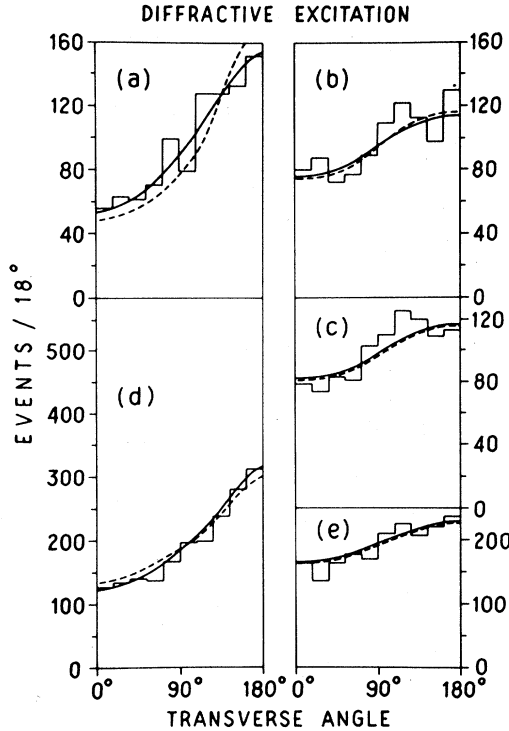


FIG. 2. Order the center-of-mass longitudinal momenta of the pions from the fastest forward to the fastest backward and label them k_2, k_3, k_4, k_5 , respectively. Let k_1 and k_6 be the center-of-mass longitudinal momenta of the forward-going and backward-going proton, respectively. Then, the transverse-angle correlations plotted (and defined in the text) are between (a) k_1 and k_6 ; (b) k_2 and k_5 ; (c) k_3 and k_4 ; (d) k_1 and k_2, k_5 and k_6 ; and (e) k_2 and k_3, k_4 and k_5 . Curves are DEM calculations.

$$\begin{aligned} C_\pi &= -2.0, \\ C_p &= -0.5, \\ a' &= a = 1.5 \end{aligned} \quad (6)$$

produce⁷

$$\begin{aligned} \langle k_{\perp} \rangle_\pi &\cong 300 \text{ MeV}, \\ \langle k_{\perp} \rangle_p &\cong 430 \text{ MeV}. \end{aligned} \quad (7)$$

The resulting contribution to the final state from double excitation, with this $|T_n|^2$, is 23%. The suppression is of course due to kinematics: the minimum momentum-transfer requirement.

Figure 2 shows various two-particle correlations in the transverse angle φ defined by

$$\cos \varphi_{ab} = \frac{\vec{k}_{\perp a} \cdot \vec{k}_{\perp b}}{|\vec{k}_{\perp a}| |\vec{k}_{\perp b}|}, \quad (8)$$

in the k_{\perp} plane transverse to the beam direction.

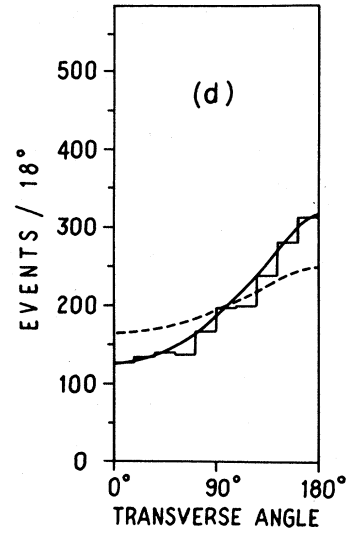


FIG. 3. Transverse-angle correlations of type (d). (See Fig. 2.) The solid curve is DEM with double excitation included and the dashed curve is DEM with single excitation only.

The solid curves are the model results when Eq. (2a) is used for the residue function, and the dashed curves when Eq. (2b) is used. The proton-proton correlations appear to be the most sensitive test of the parametrization of the residue function, but, lacking the single-particle distributions for this data, we do not know if this difference is significant.

Some versions of DEM include only single excitation in the calculations⁸: One nucleon gets excited at a time. We removed the double excitation from our calculations and found that there was little change in all the correlation distributions except for the correlation between the fast forward (backward) proton and the fast forward (backward) pion. Figure 3 shows this correlation distribution. The data clearly require the double excitation mechanism.

MULTIPERIPHERAL MODEL

The basic multiperipheral graphs included in our calculation for the data analyzed here are shown in Figure 4. Each graph has a contribution to the invariant amplitude of the form:

$$T_n = \prod_{i=1}^{n-1} \left(\frac{s_{i,i+1} + b_i}{b_i} \right)^{\alpha_i(t_{i,i+1})} e^{a_i t_{i,i+1}}. \quad (9)$$

Here $s_{i,i+1}$ is the square of the subenergy between particle i and $i+1$. α_i is either an effective meson trajectory $\alpha_M(t)$, or a baryon trajectory $\alpha_B(t)$, where

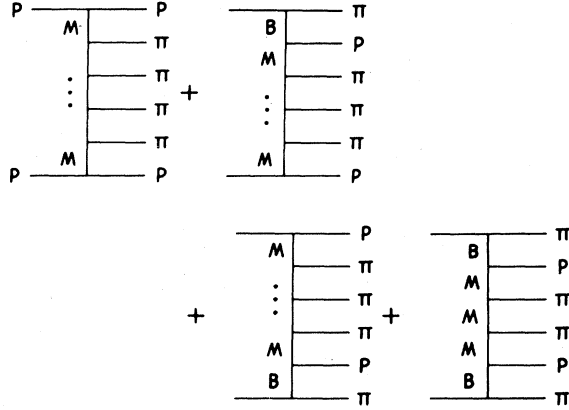


FIG. 4. The multiperipheral graphs included in this paper.

$$\begin{aligned}\alpha_M(t) &= \frac{1}{2} + t, \\ \alpha_B(t) &= -\frac{1}{2} + t.\end{aligned}\quad (10)$$

The residue functions have been parametrized as e^{at} , as usual. Also, the constants b_i are included so as to replace the Regge behavior by phase space when the subenergy of any link becomes small.

We assume isospin 1 for the meson exchange links, and no doubly charged baryon exchange links. The resulting amplitude is then symmetrized over the like particles in the final state.

For simplicity, we assume that the a_i and b_i are independent of the configuration of final particles. The values

$$a_i = 0, \quad \text{all } i$$

$$b_1 = b_5 = 2,$$

$$b_2 = b_3 = b_4 = 1,$$

produce average transverse momenta for pions and protons

$$\langle k_{\perp} \rangle_{\pi} \cong 300 \text{ MeV},$$

$$\langle k_{\perp} \rangle_P \cong 430 \text{ MeV},$$

respectively.

The graphs for meson exchange alone and those including links of baryon exchange were added with the same weight and phase. The resulting contribution from baryon exchange was $\sim 50\%$. The differential cross sections were again evaluated exactly using the numerical integration technique mentioned above.

Figure 5 shows the transverse-angle correlation data and the multiperipheral calculation. The solid curves are the results with baryon exchange

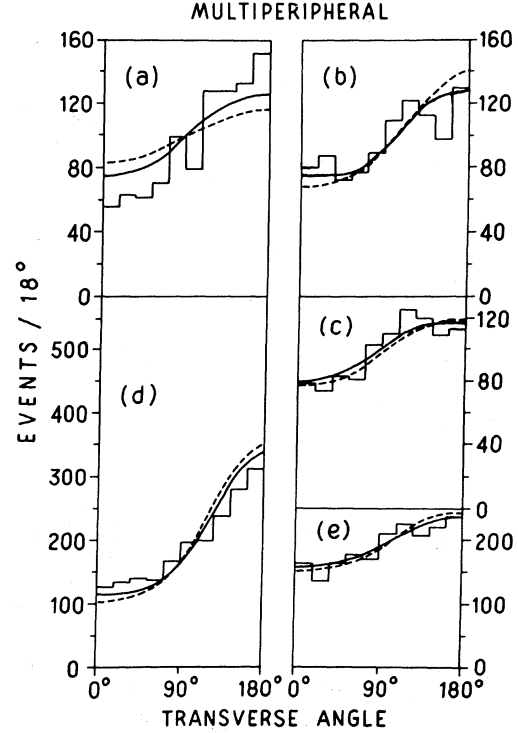


FIG. 5. Transverse-angle correlations. See Fig. 2 caption for specifics. The solid curves are the results from MPM with the nucleon-exchange graphs included and the dashed curves are the results when only meson-exchange graphs are considered.

included (see Fig. 4), and the dashed curves are the results with meson exchange alone. The proton-proton correlations [Fig. 5(a)] are obviously too weak, reflecting the fact that the multiperipheral chain has only short-range memory.

DISCUSSION

In the present situation of the investigation of strong interactions at high energy, it is preposterous to assert which is the correct theory. Both DEM and MPM seem to be able to fit the inclusive spectra, both display limiting inclusive distributions and probably scale in the Feynman sense. Both have shown a logarithmically increasing average multiplicity, although MPM more convincingly, and both can produce a constant total production cross section.

The basic difference between DEM and MPM lies in the adding-up process of the exclusive channels to the inclusive distributions. For example, in the MPM the $F(x) = x^0 dN/dx$ distribution for produced pions, where $x = 2k_{\parallel}/s^{1/2}$ and $x^0 = 2E/$

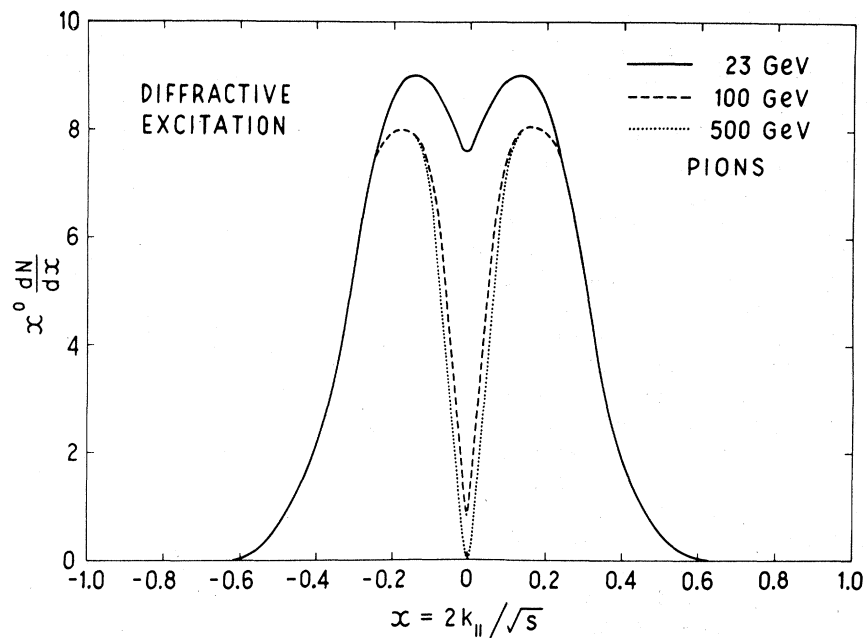


FIG. 6. Diffractive excitation model curves for $x^0 dN/dx$, where $x^0 = 2E/s^{1/2}$.

$s^{1/2}$ does *not* limit for each channel, but the channels add up to an inclusive $F(x)$ (in $p + p \rightarrow \pi + \text{anything}$) distribution that does limit. In the DEM each channel limits and the exclusive channels add up to a limiting inclusive $F(x)$ distribution.⁹

Figures 6 and 7 show our model calculations for $F(x)$ and the reaction studied here, using DEM

and MPM. The differences are obvious in this exclusive final state: One cannot miss the hole at $x \sim 0$ that DEM develops as $s \rightarrow \infty$. In the DEM studied here, the hole at $x \sim 0$ develops rapidly between 23 and 100 GeV; the distribution having developed nearly to the 100-GeV distribution by 60 GeV. There seems to be no way to avoid its

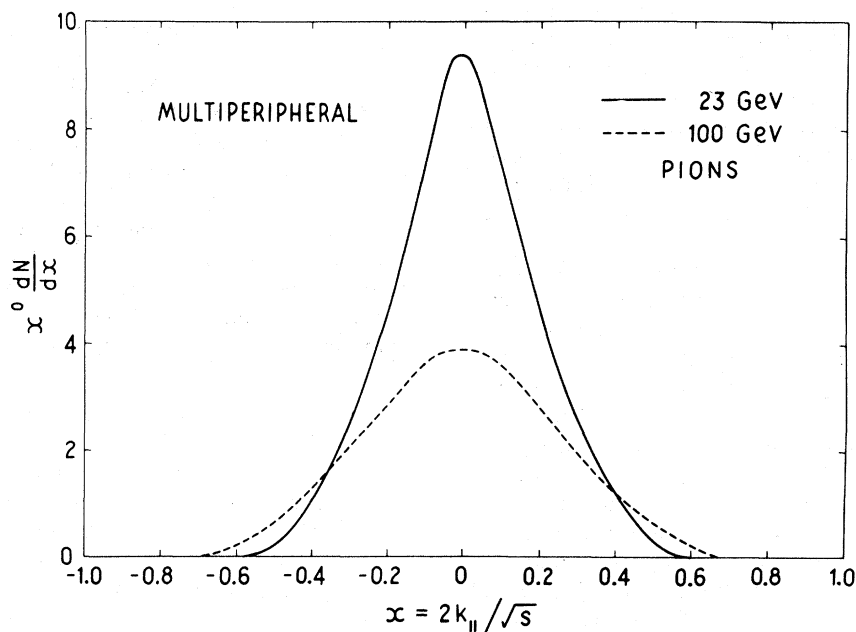


FIG. 7. Multiperipheral-model curves for $x^0 dN/dx$, where $x^0 = 2E/s^{1/2}$.

appearance in exclusive channels, other forms of the decay probability, $P_j \rightarrow n_j$, only delay its development. The MPM, however, does not have the slightest dip at $x \sim 0$.

It is relatively easy for the DEM to describe the correlation data studied in this paper. However, the MPM, even with the effects of symmetrization and baryon exchange considered here, does not reproduce the proton-proton correlations. One obvious thing to do in the MPM is to let the baryon travel further down the chain. However, the number of parameters in the model then increases and this obscures the true mechanism. It seems likely that a more promising approach for MPM is to write an amplitude that is dual in the sense that not only multi-Regge exchange effects are included but also one where cluster formation is present. This makes the effective "distance" between protons shorter, thus, increasing their correlations. Nevertheless, such proton-proton correlations diminish in the MPM with increasing s , as contrasted with the DEM.

Because of the simplifying assumptions made here for DEM, which led to Eqs. (1) and (2), the model predicts an isotropic distribution of the final products in the azimuth angle, ϕ , around the fireball direction; i.e., s -channel helicity. This is, alas, not the experimental situation.¹⁰ To study this result in the pp reaction one takes the fastest final-state proton, in the center-of-mass system, and considers it to be the unexcited proton. Then the "fireball" direction, taken to be the direction opposite the unexcited nucleon, is used to plot such an azimuth-angle distribution. Figure 8 shows this plot for the final state considered here. The two models differ most for the nucleon from the "fireball" decay. We note that the asymmetry in DEM is due entirely to the presence of double excitation in the model and the error that results in determining the "fireball" direction when plotting the final state in the manner prescribed above.

Because of the statistical nature of the decay in DEM, it is not clear how angular momentum coupling of the participating particles can be incorporated. In addition, we know that final-state interactions must be present and invalidate the factorizable Pomeranchukon assumption. How to take these effects into account is complicated, if not unknown. Helicity plots for exclusive final states would help. Further, DEM predicts that various components of an isomultiplet have the same $d\sigma/d\alpha$ distributions. Discrepancies can reveal the goodness of the statistical postulate and the strengths of resonance and final-state inter-

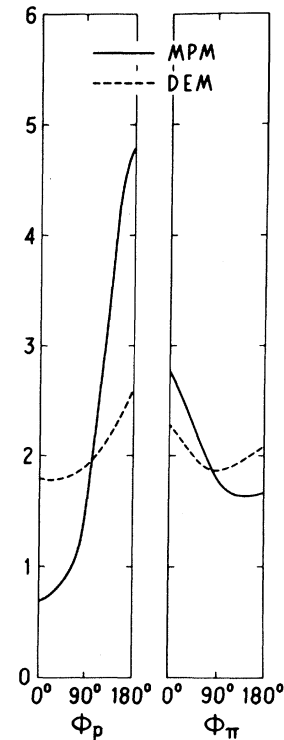


FIG. 8. s -channel helicity for MPM (solid curves) and DEM (dashed curves), for the proton from the excited nucleon decay, ϕ_p , and the pions from the excited nucleon decay, ϕ_π . See text for definition of "excited nucleon."

actions in a fireball.

CONCLUSIONS

At 23 GeV/c the DEM fits the correlation data studied here with relative ease. The MPM can fit all satisfactorily except the p - p correlations. The energy dependence is crucial, however, and should be studied. Further, we have demonstrated that various projections of the exclusive final state are quite different in the two models, whereas the inclusive projections are much the same. The modern tendency to plot inclusive distributions alone, therefore, should be avoided.

ACKNOWLEDGMENTS

We would like to thank Professor R. C. Hwa, Professor M. Ross, Professor J. VanderVelde, and Mr. W. Cooper for many discussions. To J. V. V. and W. C., we are particularly grateful for making available to us their unpublished $d+p$ data.

¹For example, G. F. Chew and A. Pignotti, *Phys. Rev.* **176**, 2112 (1968).

²For review see R. C. Hwa, Davis International Conference on Inclusive Reactions, 1972 (unpublished).

³D. B. Smith, Ph.D. Thesis, LBL Report No. UCRL-20632, 1971 (unpublished). J. H. Friedman, C. Risk, and D. B. Smith, *Phys. Rev. Letters* **28**, 191 (1972).

⁴This factor is somewhat arbitrary here since one invokes f dominance only after all the decays of a fireball have been summed over, and since it is impossible to determine precisely how this dynamical assumption should be distributed among the decay states.

⁵J. H. Friedman, *Journal of Comput. Phys.* **7**, 201 (1971).

⁶The statistical accuracy of the Monte Carlo calculations was $\sim 0.1\%$.

⁷If we compare Eq. (6) with Eq. (7), we see that the values of C_π and C_p bear little resemblance to $\langle k_\perp \rangle_\pi$ and $\langle k_\perp \rangle_p$ respectively.

⁸M. Jacob and R. Slansky, *Phys. Rev. D* **5**, 1847 (1972). We should mention, however, that more recent calculations in the "nova model" allow for double excitation.

⁹R. C. Hwa and C. S. Lam, *Phys. Rev. Letters* **27**, 1098 (1971); R. C. Hwa, *Phys. Rev. Letters* **26**, 1143 (1971).

¹⁰At least it is not the case in the process $d+p \rightarrow d+p+\pi^++\pi^-$. In fact here MPM provides a satisfactory fit to the helicity plots.

PHYSICAL REVIEW D

VOLUME 6, NUMBER 11

1 DECEMBER 1972

Azimuthal Correlations of High-Energy Collision Products

Margaret C. Foster, Daniel Z. Freedman, and S. Nussinov*

*Department of Physics and Institute for Theoretical Physics,
State University of New York at Stony Brook,† Stony Brook, New York 11790*

and

J. Hanlon and R. S. Panvini

Vanderbilt University, Nashville, Tennessee‡ 37203

(Received 24 July 1972)

Experimental distributions of azimuthal angles between particles produced in pp and pd collisions at 28 GeV/c and K^-p collisions at 9 GeV/c are presented and studied. A simple protostatistical model describes the over-all azimuthal distributions quite well. Other models are also considered. We show that the azimuthal distribution for reactions of fixed charged prong number may be used to estimate the average number of missing neutrals, and we study the distributions of a collective variable designed to test for a preferred transverse direction in multiparticle events.

I. INTRODUCTION

The study of two-particle correlations is a natural step beyond the investigation of single-particle distributions.^{1,2} Such a study could be very useful in clarifying our understanding of multiple-particle production in high-energy collisions.

In this paper we concentrate on azimuthal correlations, that is, distributions $d\sigma/d\phi_{ij}$ where ϕ_{ij} is the angle between transverse momenta \vec{k}_i and \vec{k}_j of two final-state particles. Experimental azimuthal distributions have been studied previously^{3,4} and their theoretical significance in inclusive reactions has been discussed.⁵ The data of three AGS 80-in. BNL bubble-chamber experiments on pp and pd collisions at⁶ about 28 GeV/c and K^-p collisions at⁷ 9 GeV/c are studied. The following kinematically fitted reactions are used: pp

$\rightarrow pp\pi^+\pi^-$, $pp\pi^+\pi^-\pi^+\pi^-$ at 28.5 GeV/c; $pd \rightarrow (p_s)pp\pi^-\pi^-\pi^+$ at 28.0 GeV/c; and $K^-p \rightarrow K^-p\pi^+\pi^-$, $K^-p\pi^+\pi^-\pi^+\pi^-$, $K^-p\pi^+\pi^-\pi^+\pi^-\pi^+$ at 9 GeV/c. Unfitted events with between two and ten prongs in pp collisions and between two and eight prongs in K^-p collisions are also treated.

The main goal of our study is to identify the correlations which arise simply from momentum conservation and the experimentally observed damping of transverse momenta. A general prediction of the momentum conservation constraint is discussed in Sec. II.

In Sec. III, we suggest a "protostatistical" distribution which incorporates transverse-momentum conservation and damping and compares rather well with the over-all experimental distributions

$$\frac{d\sigma^n}{d\phi} \equiv \sum_{i \neq j} \frac{d\sigma^n}{d\phi_{ij}},$$